A critical examination on the use of pseudopotentials in the inelastic atomic collision theory

xxx, xxx, xxx and J. E. Miraglia

Instituto de Astronomía y Física del Espacio (IAFE, UBA-CONICET)

Consejo Nacional de Investigaciones Científicas y Técnicas and

Departamento de Física. Facultad de Ciencias Exactas

y Naturales. Universidad de Buenos Aires. Argentina.

(Dated: August 2, 2018)

Abstract

We explore the possibility of using pseudo potentials within the single electron model to calculate inelastic transitions. Single photoionization, excitation, ionization and electron capture were calculated in first perturbative order. We conclude that the range of validity is restrained to very small momentum transfers.

PACS numbers: 34.10.+x,34.80.Dp,34.70.+e

I. INTRODUCTION

Most of the scientific community have recognized that the use of the Density Functional Theory (DFT) has revolutionized the development of atomic and molecular physics [1]. However it is the tandem of the DFT along with the use of pseudopotentials (PPs) that have motorized the field even further, permitting to tackle huge molecules that otherwise would have been intractable [2, 3, 5].

For our purpose, one great advantage of the PPs is that they avoid the complexity of the wave function near the core that normally consumes a huge numerical effort. For instance codes using DFT+PPs, such as the PARSEC for example [4], permit to use an equally-spaced grid involving a relatively small number of points. Otherwise, if we use realistic potentials describing the proper nucleus Coulomb potential, a high density of points concentrated at the origin is required to describe precisely what the PPs cast aside. It is our idea that if PPs work in our field of collisions theory, we could save up to one order of magnitude in the amount of points in the spatial grid. That would be an enormous advantage which would let us engage with more sophisticated methods.

This article pretends to answer the following question: To what extend ca n we use PPs in the atomic collision theory to describe inelastic transitions at intermediate-high impact velocities? We are interested in inelastic collisions involving a single electron transition, namely: excitation, ionization and electron capture. To get to the point, we will make several simplifications:

a) We will restrain the calculation to a (pseudo) Hamiltonian $\widehat{H}$ dealing with only three particles, i.e. a moving projectile, a target and the active electron

$$\widehat{H} = \widehat{K}_P + \widehat{K}_e + V_{Pe} + V_{Te}, \tag{1}$$

where $\widehat{K}_P$ ($\widehat{K}_e$) is the projectile (electron) kinetics energy operator, and V_{Pe} (V_{Te}) is the projectile-electron (target-electron) potential.

b) As we deal with an active electron, we will tackle atoms with a single outer electron, namely H(1s) and Li(2s). This choice avoids any further complication involving the interelectronic interactions.

c) We will consider local PPs corresponding to the same angular momentum of the initial state, i.e. $l = 0$ in our case.

d) We will compare with the standard calculation in atomic collision where V_{Pe} and V_{Te} are obtained with the Depurated Inversion Method (DIM) of the numerical Hartree Fock orbitals [6, 7].

e) We will concentrate in the calculation of the first perturbative order of the T-matrix element corresponding to the transition under study. Except electron capture, the first order using Hartree Fock orbitals provides the correct high energy limit. We start from the premise that if the PP fails to describe the first order, it will certainly also fail when calculating a higher order or a distorted wave such as the Continuum Distorted Wave, Impulse Approximation, etc., normally used to extend the energy range of validity.

To facilitate the comprehension of the different models, we use here the following notation:

i) When we write *normal capital* letters, H(1s) or Li(2s), we consider the electron bound to the nucleus described with the best Hartree Fock potential by using the DIM, as used routinely in the single particle inelastic collision theory. For H(1s) we obviously refer to the pure Coulomb potential, and for Li(2s) we use the sum of generalized static potentials (see Eq.(4) below).

ii) We use *calligraphic capital* letters, $\mathcal{H}(1s)$ or $\mathcal{L}i$, to represent that the electron is bound to the nucleus through a pseudopotential.

We are going to explore 3 PPs extracted from 3 popular sites that we denote by P (from Parsec home page), Q (from Quantum Express), and A (from Abinit). Files and references are in Table [12]

PP	Type	file	Ref.
P	Troullier Martins,	H_POTRE.DAT, Li_POTRE.DAT.	[9]
Q	blyp, Vanderbilt,	H.blyp-van_ak.UPF.dat	[8]
A	GGA PBE,	01-H.GGA.fhi.txt, 03-Li.GGA.fhi.txt.	[10]

.

In all cases we solve the radial Schrodinger equations with RADIALF code [11]. Atomic units are used.

A. Potentials

Any "realistic" local atomic potential describing a single-particle orbital model could be cast in the form

$$V(\overrightarrow{r}) = -\frac{Z_r(r)}{r}, \quad / \quad Z_r(r) \rightarrow \begin{cases} 1, & r \rightarrow \infty \\ Z_n, & r \rightarrow 0 \end{cases}; \tag{2}$$

where Z_n is the nuclear charge, and its Fourier transform $\widetilde{V}$ reads

$$\widetilde{V}(\overrightarrow{k}) = -\sqrt{\frac{2}{\pi}}\frac{Z_k(k)}{k^2}, \quad / \quad Z_k(k) \rightarrow \begin{cases} 1, & k \rightarrow 0 \\ Z_n, & k \rightarrow \infty \end{cases}. \tag{3}$$

For hydrogen, we have simply $Z_r(r) = Z_k(k) = 1$. For $Li(2s)$ we have obtained $Z_r(r)$ by using the Depurated Inversion Method (DIM) from the Hartree Fock solutions [6, 7], and it was fit with a sum of generalized static potentials as follows

$$Z_r(r) = 1 + \sum_{j=1}^{3} Z_j e^{-\beta_j r}(1 + \alpha_j r), \tag{4}$$

so that $\Sigma_j Z_j = 2$. The counterpart, in the Fourier space reads

$$Z_k(k) = 1 + \sum_{j=1}^{3} Z_j \frac{k^2(k^2 + \beta(2\alpha_j + \beta_j)}{(k^2 + \beta_j^2)^2}, \tag{5}$$

and their results are shown in Figures 2a and 2b.

A PP introduces a cut off in the core region ($r < r_c$)

$$V_{PP}(\overrightarrow{r}) = -\mathcal{Z}_r\left(\frac{r}{r_c}\right)\left(\frac{1}{r}\right), \tag{6}$$

$$\mathcal{Z}_r\left(\frac{r}{r_c}\right) = \begin{cases} 1, & r > r_c \\ \left(\frac{r}{r_c}\right)^{\alpha}, & r \rightarrow 0, \end{cases}, \tag{7}$$

so that V_{PP} renders a nodeless wave function having the proper eigenenergy of the corresponding orbital. For $\alpha > 2$, V_{PP} vanishes at the origin avoiding the Coulomb potential, but it has a price: $\widetilde{V}_{PP}(k)$ does not represent the proper nuclear Coulomb potential for $k > r_c^{-1}$ but a quite erratic behavior; oscillatory in most of the cases.

Effective charges $\mathcal{Z}_r$ and $\mathcal{Z}_k$ are shown in Figures 1a/b and 2a/b. One expects that the smaller the cut off r_c, the larger will be the range of validity in the k-space which can be estimated to be of the order of r_c^{-1}.

For Hydrogen, the Troullier Martins PP uses the smaller cut off, $r_P = 0.15$, and so the larger will be the range of validity in the k-space. Departure from unity is observed for $k > 6r_P^{-1}$. The cut offs for PPs A and Q, instead, are around unity ($r_A = 1.27$ and $r_Q = 0.82$) and therefore their ranges diminish appreciably in k-space. However, by construction, PP A remains near unity up to $k \simeq 5$, while Q PP keeps near unity up to $k \simeq 3$ only. The Vanderbilt technique produces a desirable smoothness in the r-space but, on the contrary, it departures very rapidly and uniformly from the unity in the k-space. The r-space softness will not be here necessarily a quality to attain: As we shall see, the k-space behavior rules the success in inelastic collisions.

For Li(2s), as shown in Figure 2, both PP A and P cut offs are similar $r_c \simeq 2.3$, and so no appreciable difference is observed in $r-$ and $k-$space. The important feature to observe is that for $k > 1$ both vanish with an oscillatory behavior, changing of sign: for momentum transfer around $k \approx 2$, the PP behaves unacceptably like an antiproton.

B. Wave Functions

If we write the solution of the Schrodinger equation as usual, $\psi_{mlm}(\overrightarrow{r}) = u_{nl}(r)/r\ Y_l^m(\widehat{r})$, its Fourier transform can be expressed as

$$\widetilde{\psi}_{nlm}(\overrightarrow{k}) = \frac{\chi_{nl}(k)}{k} Y_l^m(\widehat{k}). \tag{8}$$

Function $u_{nl}(r)$, and $\chi_{nl}(k)$ are displayed in Figures 1d and 2d.

For Hydrogen, as expected, the Troullier Martins PP describes perfectly the function in k-space, while A and Q Fourier functions reproduce the success of the corresponding PPs.

For Li there is an interesting point to remark: Even though the pseudo wave function is nodless, which can be associated to a typical 1s state ground state, its Fourier transform has a node, resembling the 2s wave function instead. However for values of k larger than the node, discrepancies with the Hartree Fock functions are large. In Figure 2d we have single out this region by multiplying the ordinate by 10 to be well observed the difference. This failure will introduce devastating consequences at the level of cross sections.

II. COMPARISONS

In this section we will compare Hartree Fock potentials, wave functions, and cross sections corresponding to four inelastic processes: photoionization, excitation, ionization and electron capture.

A. Single Photoionization

The simplest inelastic process is the photoionization where the initial bound (ψ_i) as well as the final continuum ($\psi^-_{\overrightarrow{k}_f}$) states are not appreciably distorted as far as the photon field is perturbative. The relevant matrix element is in atomic units

$$T^{ph}_{\overrightarrow{k}} = \int d\overrightarrow{r}\ \psi^-_{\overrightarrow{k}_f}(\overrightarrow{r})\ \left(-i\ \widehat{\varepsilon}_\lambda \cdot \overrightarrow{\nabla}_{\overrightarrow{r}}\right)\ \psi_i(\overrightarrow{r}), \tag{9}$$

$\widehat{\varepsilon}_\lambda$ is the polarization versor, and $k_f = \sqrt{2(\omega + \varepsilon_i)}$ as imposed by the energy conservation. For pure hydrogen

$$ph + H(1s) \rightarrow H^+ + e, \tag{10}$$

the wave function is well known from the origin of quantum mechanics, and the integrals to obtain $T^{ph}_{\overrightarrow{k}}$ can be found in any text book. A relevant magnitude of the hydrogenic continuum state is the enhancement factor E that in this case is reduced to the so-called Coulomb factor

$$E\ =\ \left|\psi^-_{\overrightarrow{k}_f}(0)\right|^2 = \frac{2\pi Z/k_f}{1-\exp(-2\pi Z/k_f)} \underset{k_f\rightarrow\infty}{\rightarrow} 1, \tag{11}$$

$$\underset{k_f\rightarrow 0}{\rightarrow} \begin{cases} +\infty, & \text{for } Z > 0 \ \text{ (electrons)} \\ 0, & \text{for } Z < 0 \ \text{ (positrons)} \end{cases}. \tag{12}$$

The photoionization of one electron in pseudohydrogen

$$ph + \mathcal{H}(1s) \rightarrow \mathcal{H}^+ + e, \tag{13}$$

is no longer a Coulombian issue. We recall that we use calligraphic letters to indicate the atom interacting via PP. Thus, to obtain the PP enhancement factor we need to solve numerically the corresponding Schrodinger equation for the continuum state $\phi^-_{\overrightarrow{k}_f}$ of the corresponding PP, and to do

$$E = \left|\phi^-_{\overrightarrow{k}_f}(0)\right|^2. \tag{14}$$

In Figure 3a we compare the hydrogenCoulomb factor against the one provided by the PPs. Notably the performance of the Troullier Martins potential is superb not only to describe the enhancement factor for electrons but for positrons as well. But for the Li case, as shown in Figure 3b, we have a complete different scenario: the PPs fail to describe the Hatree Fock enhancement factors. They trespass unity, which means that electrons behave as positrons instead, as a consequence of the change of sign, as observed in Figure 2b.

Photoionization cross sections are displayed in Figure 4. For hydrogen, A and Q PPs work at small photon energies, failing at larger ejecting electron energies. The explanation is simply restrained to the behavior in Fourier space of the pseudowave functions. If we consider, very roughly, that $\psi^{-}_{k_f}(\overrightarrow{r})$ can be approximated by a plane wave, the element $T^{ph}_{\overrightarrow{k}}$ can be reduced to

$$T^{ph}_{\overrightarrow{k}} \sim -\left(\widehat{\varepsilon}_\lambda \cdot \overrightarrow{k}_f\right)\ \widetilde{\psi}_i(\overrightarrow{k}_f). \tag{15}$$

The larger the photon energy, the larger the k_f, entering so in the conflicting region of $\widetilde{\psi}_i$. For Hydrogen, the Toullier Martins PP magnifically represents the photoionization as a simple consequence of the proper description of the Fourier transform of the initial state. For $Li(2s)$ and its PPs counter part $\mathcal{L}i$, the disagreement is more than evident: It simply replicates the oscillatory structure of the wave functions observed in the large k-space.

B. Single Excitation

Let us consider the simplest excitation process in first perturbative order and compare the results with the ones obtained using PPs

$$\begin{cases} H^+ + H(1s) \rightarrow H^+ + H(n=2,3), \\ \mathcal{H}^+ + \mathcal{H}(1s) \rightarrow \mathcal{H}^+ + \mathcal{H}(n=2,3), \end{cases} , \tag{16}$$

as shown in Figure 5a. The first Born Transition matrix element for this direct process is given by

$$T^{B1}_{fi} = \widetilde{V}(\overrightarrow{p}) F_{fi}(\overrightarrow{p}). \tag{17}$$

The term $F_{fi}(\overrightarrow{p})$ is the well known form factor

$$F_{fi}(\overrightarrow{p}) = \frac{1}{(2\pi)^{3/2}} \int d\overrightarrow{k}\ \widetilde{\psi}^*_f(\overrightarrow{k})\ \widetilde{\psi}_i(\overrightarrow{k} + \overrightarrow{p}), \tag{18}$$

$\overrightarrow{p}$ is the momentum transfer vector

$$\overrightarrow{p} = p_{\min}\widehat{v} + \overrightarrow{\eta}, \tag{19}$$

$$p_{\min} = \frac{\varepsilon_f - \varepsilon_i}{v} \rightarrow \begin{cases} \infty, & v \rightarrow 0 \\ 0, & v \rightarrow \infty \end{cases}, \tag{20}$$

$\overrightarrow{v}$ is the ion velocity and $\overrightarrow{\eta}$ is the transversal momentum transfer, so that $\widehat{v} \cdot \overrightarrow{\eta} = 0$, and $\varepsilon_i(\varepsilon_f)$ is the initial (final) binding energy corresponding to the state ψ_i (ψ_f).

For the simplest hydrogenic case (16) the element of matrix T_{fi}^{B1} has a well known closed form, but for the pseudopotentials we need to solve the radial Schrodinger equation in a given grid and integrate it numerically (20). By doing so we warrant the full orthonormality $\langle\psi_f|\psi_i\rangle = \delta_{if}$.The results are displayed in .Figure 5a. The performance of A and P PPs are superb, but Q PP fails, and one reason is that $\varepsilon_i = -0.4522$ does not agree well with the hydrogen one, -0.50. As T_{fi}^{B1} through $\widetilde{V}(\overrightarrow{p})$ depends strongly on $p_{\min}$ and so on $\Delta\varepsilon = \varepsilon_f - \varepsilon_i$; a failure on $\Delta\varepsilon$ magnifies the errors.

In Figure 5b we compare the next system

$$\begin{cases} Li^+ + Li(2s) \rightarrow H^+ + H(n = 2p,\ n = 3), \\ \mathcal{L}i^+ + \mathcal{L}i(1s) \rightarrow \mathcal{L}i^+ + \mathcal{L}i(n = 2,\ n = 3), \end{cases}, \tag{21}$$

corresponding to the potentials displayed in Figure 2b. In this comparison there is a very important point to note. As the wave function has no nodes, the PP describes the $2s$ of Lithium as 1s nodless ground state, $\mathcal{L}i(1s)$, therefore $n = 2$ involves both $2p$ and $2s$ final state, while for $Li(2s)$ it involves excitation to $2p$ alone.

We have some agreement only at high impact energy where $p_{\min} \rightarrow 0$. At intermediate energies the PPs fail and this is because of the bad behavior of $\widetilde{V}(\overrightarrow{p})$ for moderate values of $p_{\min}$, as shown in Figure 2b. We can test this interpretation by removing the ill behavior of $\mathcal{Z}_k(p)$ by considering a bare impinging proton characterized with a precise Coulomb charge $Z_k = 1$, representing the colliding systems

$$\begin{cases} H^+ + Li(2s) \rightarrow H^+ + Li(2p,\ n = 3) \\ H^+ + \mathcal{L}i(1s) \rightarrow H^+ + \mathcal{L}i(n = 2,\ n = 3) \end{cases}. \tag{22}$$

Clearly the performance of the pseudopotentials improves notably, however still a failure at lower velocities is observed, but in this case the source comes from the form factor, as

explained next. An alternative expression for the form factor can be obtained by using the peaking approximation to obtain

$$F_{fi}(\overrightarrow{p}) \sim \widetilde{\psi}_i(\overrightarrow{p})\psi_f^*(0) + \widetilde{\psi}_f^*(\overrightarrow{p})\psi_i(0). \tag{23}$$

It becomes now clear that an incorrect behavior of $\widetilde{\psi}_i(\overrightarrow{p})$ at large values of p (see Figure 2d) will cast erroneous form factors.

C. Single Ionization

In Figure 6 we study the single differential ionization cross section in energy $d\sigma/d\varepsilon_f$ for the impact of a projectile impinging with $v = 1$ (25 keV/amu), for the same systems as in Figure 5. In first Born approximation the Transition matrix reads the same as in Eq.(18) with $\psi_f(\overrightarrow{r}) = \psi_k^-(\overrightarrow{r}), i.e.$ the outgoing continuum wave function, and $\varepsilon_f = k_f^2/2$. The performance of the PPs are equivalent to the ones of excitation. If we again consider, very roughly, that $\psi_k^-(\overrightarrow{r})$ can be approximated by a plane wave, the form factor can be reduce to the Fourier transform of the initial state

$$F_{\overrightarrow{k}_f\ i}(\overrightarrow{p}) \sim \widetilde{\psi}_i(\overrightarrow{p} - \overrightarrow{k}_f), \tag{24}$$

and we have here two source of problems: first as $v \to 0$, $p_{\min} \to \infty$, and so the PPs do not describe properly $\widetilde{\psi}_i(\overrightarrow{q})$, for large value of q. And second, as k_f increases so $p_{\min} = (k_f^2/2 - \varepsilon_i)/v$ increases as well and again $\widetilde{\psi}_i$ fails in this limit. To remove the uncertainties of $\widetilde{V}_{PP}(\overrightarrow{p})$, in Figure5c where we plot the results by proton impact. In this case the failure of the form factor in the one that remains.

D. Single Charge exchange

Finally we study the charge exchange process for the paradigmatic system

$$\begin{cases} H^+ + H(1s) \to H(1s) + H^+ \\ \mathcal{H}^+ + \mathcal{H}(1s) \to \mathcal{H}(1s)^+ + \mathcal{H}^+ \end{cases}. \tag{25}$$

In Figure 7a we show the theoretical cross sections calculated with the first order Brinkman Kramers. Its matrix element is given by

$$T_{fi}^{BK} = \widetilde{\varphi}_f^*(\overrightarrow{W}_f)\left[\varepsilon_f - \frac{W_f^2}{2}\right]\widetilde{\varphi}_i(\overrightarrow{W}_i), \tag{26}$$

and arising two momentum transfer vectors

$$\overrightarrow{W}_i \;=\; W_{i0}\widehat{v} + \overrightarrow{\eta}, \quad W_{i0} = \frac{v}{2} - \frac{\varepsilon_f - \varepsilon_i}{v}, \tag{27}$$

$$\overrightarrow{W}_f \;=\; W_{f0}\widehat{v} - \overrightarrow{\eta}, \quad W_{f0} = \frac{v}{2} + \frac{\varepsilon_f - \varepsilon_i}{v}, \tag{28}$$

satisfying the condition: $\overrightarrow{W}_i + \overrightarrow{W}_f = \overrightarrow{v}$. The performance of the PPs are superb not only for proton hydrogen but also for the Lithium case as shown in Figure 7b for $v < 1$. However these agreements are misleading because we are treating resonant charge transfer, i.e. when $\varepsilon_f = \varepsilon_i$. For any other non resonant transition $\varepsilon_f \neq \varepsilon_i$, the second summands of W_{i0} and W_{f0} are different of zero and W_i and W_f diverge as $v \to 0$. And this is clearly shown in Figure 7c where we consider the impact of a pure hydrogenic projectile

$$\begin{cases} H^+ + Li(2s) \to H(1s) + Li^+ \\ H^+ + \mathcal{L}i(1s) \to H(1s) + \mathcal{L}i^+ \end{cases}, \tag{29}$$

the first order fails completely at low and large velocities. There is one point around $v = 0.77$ where the PPs give reasonable results. And this is because $W_{f0} = 0$ and $W_{i0} = v_0$ is the minimum value, and falls within the region of validity of the Fourier transform of for the state $\mathcal{L}i$ as shown in Figure 2d

III. CONCLUSIONS

After examining the performance of the PPs to calculate inelastic cross sections we cannot recommend their use in atomic collisions in general, except when the momentum transfers be small enough. The PPs hold for the purpose that were created, only valid at large distances necessary to describe the chemical bonding, any attempt to extend their usefulness lead us to incorrect behaviors. A new kind of pseudopotential could be created to be use for inelastic collision from a different starting point. As the chemistry develops the PPs in the r-space at large distances, in the field of inelastic transitions should developed the PPs in the k-space within the region of momentum transfer of interest. And this strategy leads to a *cul de sac,* because it doest not necessarily avoids the complexity of the wave function near the core that was the original purpose

References

[1] W. Kohn and L.J. Sham, Self-Consistent Equations Including Exchange and Correlation Effects, Phys. Rev. **140**, 1133-1138 (1965).

[2] D. R. Hamann, M. Schlüter, and C. Chiang, Norm-Conserving pseudopotentials, Phys. Rev. Lett. **43**, 1494-1497 (1979).

[3] D. Vanderbilt, Soft self-consistent pseudopotentials in a generalized eigenvalue formalism,, Phys. Rev. B **41**, 7892 (1990).

[4] Leeor Kronik, Adi Makmal, Murilo L. Tiago, M. M. G. Alemany, Manish Jain, Xiangyang Huang, Yousef Saad, and James R. Chelikowsky, PARSEC – the pseudopotential algorithm for real-space electronic structure calculations: recent advances and novel applications to nano-structures, phys. stat. sol. (b) **243**, 1063–1079 (2006).

[5] N. Troullier and J. L. Martins, Efficient pseudopotentials for plane-wave calculations, Phys. Rev. B **43**, 1993 (1991).

[6] A.M.P. Mendez, D.M. Mitnik, and J.E. Miraglia, Depurated inversion method for orbital-specific exchange potentials, Int. J. Quantum. Chem. 116, 1882 (2016).

[7] Alejandra M.P. Mendez, Dario M. Mitnik, and Jorge E. Miraglia, Local Effective Hartree-Fock Potentials Obtained by the Depurated Inversion Method, Novel Electronic Structure Theory: General Innovations and Strongly Correlated Systems, (Serial Title: Advances in Quantum Chemistry, Vol. 76), p. 117-131 (2018).

[8] http://www.quantum-espresso.org/wp-content/uploads/upf_files/H.blyp-van_ak.UPF.

[9] http://parsec.ices.utexas.edu/styled-2/.

[10] ftp://ftp.abinit.org/pub/abinitio/Psps/GGA_FHI.

[11] F. Salvat, J.M. Fernandez-Varea, W. Williamson Jr., Accurate numerical solution of the radial Schrödinger and Dirac wave equations, Comput. Phys. Commun. **90** 151-168 (1995).

[12] We did not find the equivalent file, Li.blyp-van_ak.UPF.dat for Lithium.

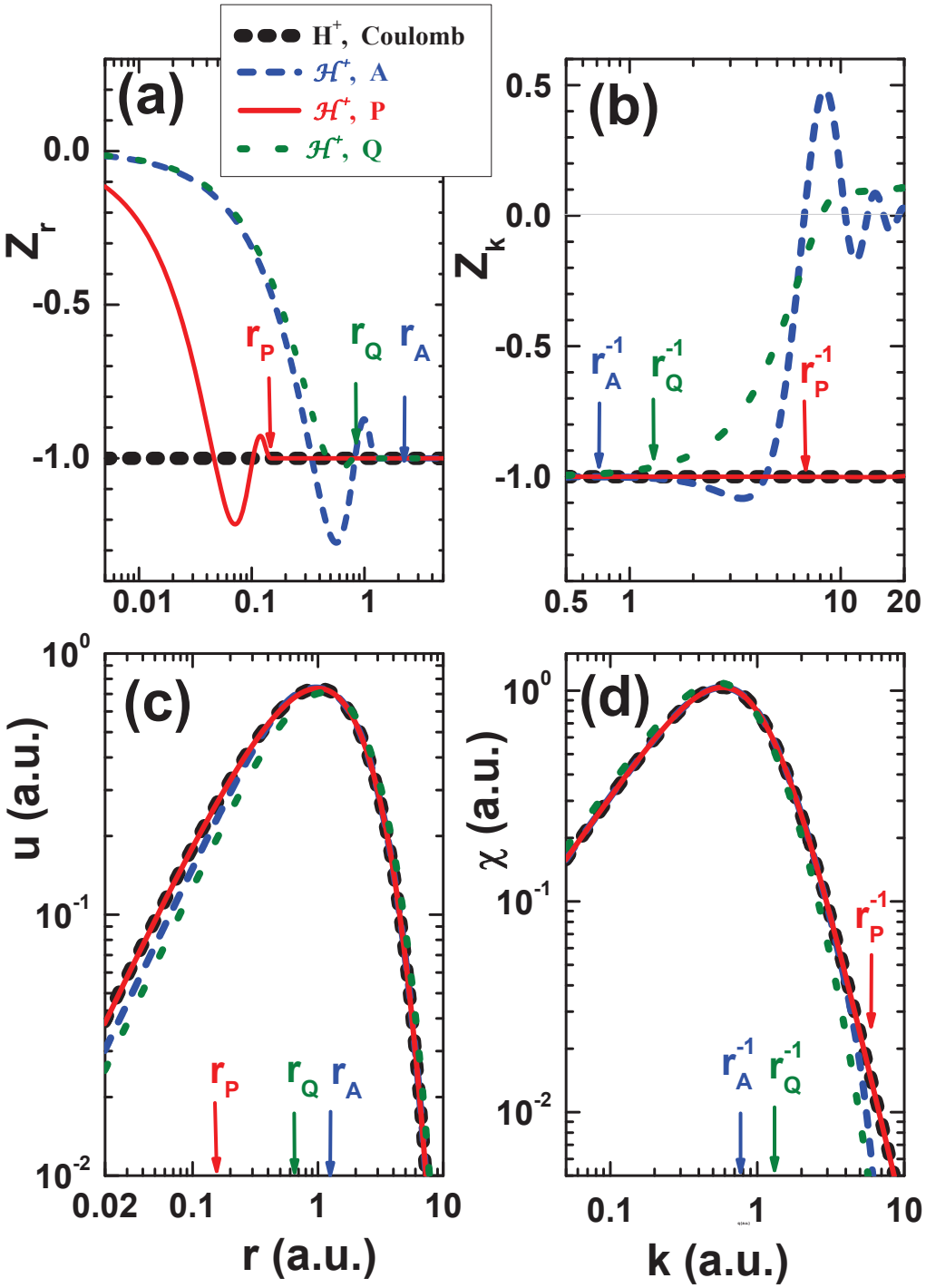

FIG. 1: (Color online) Hydrogen Coulomb and pseudo potential in real (a) and in Fourier space (b). Exact ground state for hydrogen along with the pseudo wave function in real **(c)** and Fourier space (d)

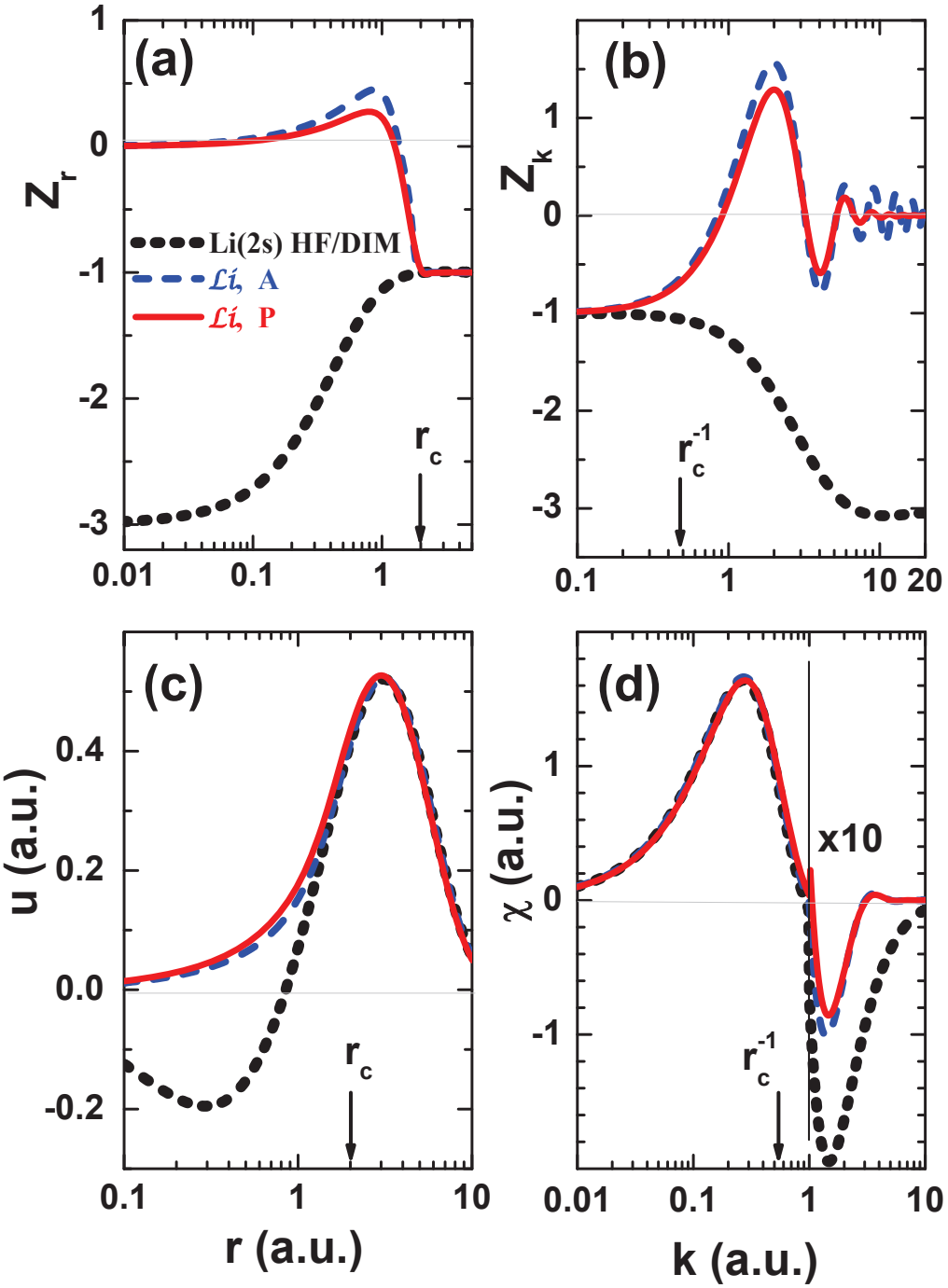

FIG. 2: (Color online) Li(2s) DIM potential and the pseudo potential in real (a) and in Fourier space (b). Hartree Fock ground state for Li(2s) along with the pseudo wave function in real **(c)** and Fourier space (d).

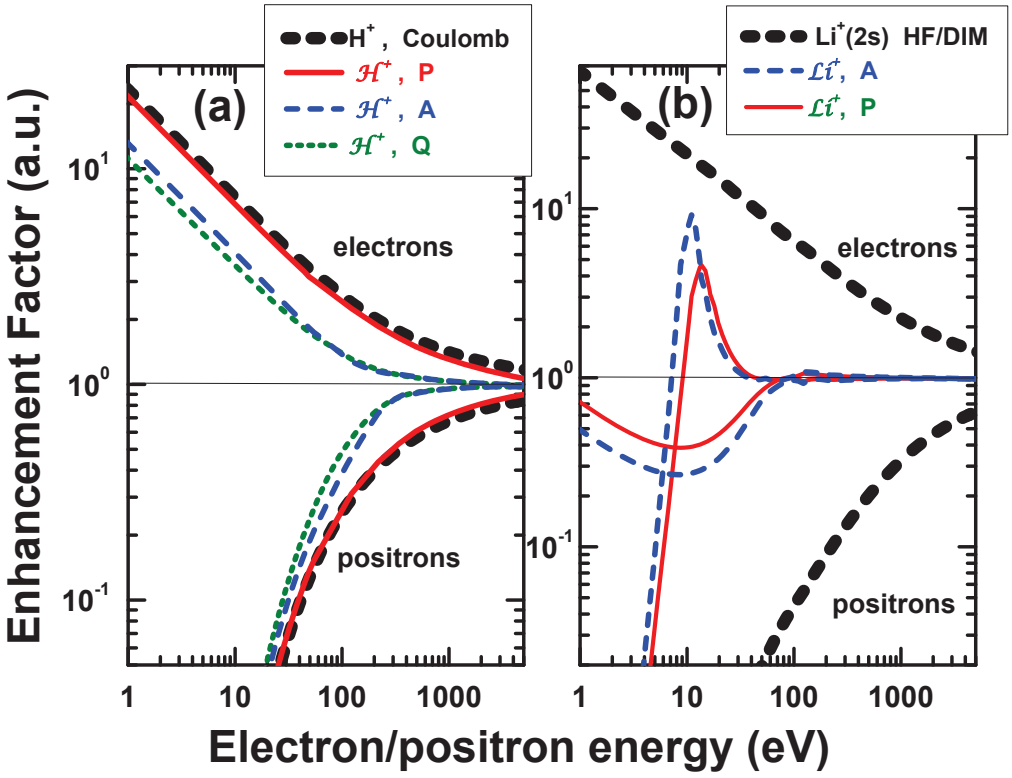

FIG. 3: (Color online) (a) Coulomb enhancement factor as given by Eq.(11) for electrons and positrons in the bare hydrogen field along with the ones calculated with pseudo potentials. (b) Enhancement factors obtained in the field of a DIM potential for electrons and positrons and the corresponding to the PP as indicated.

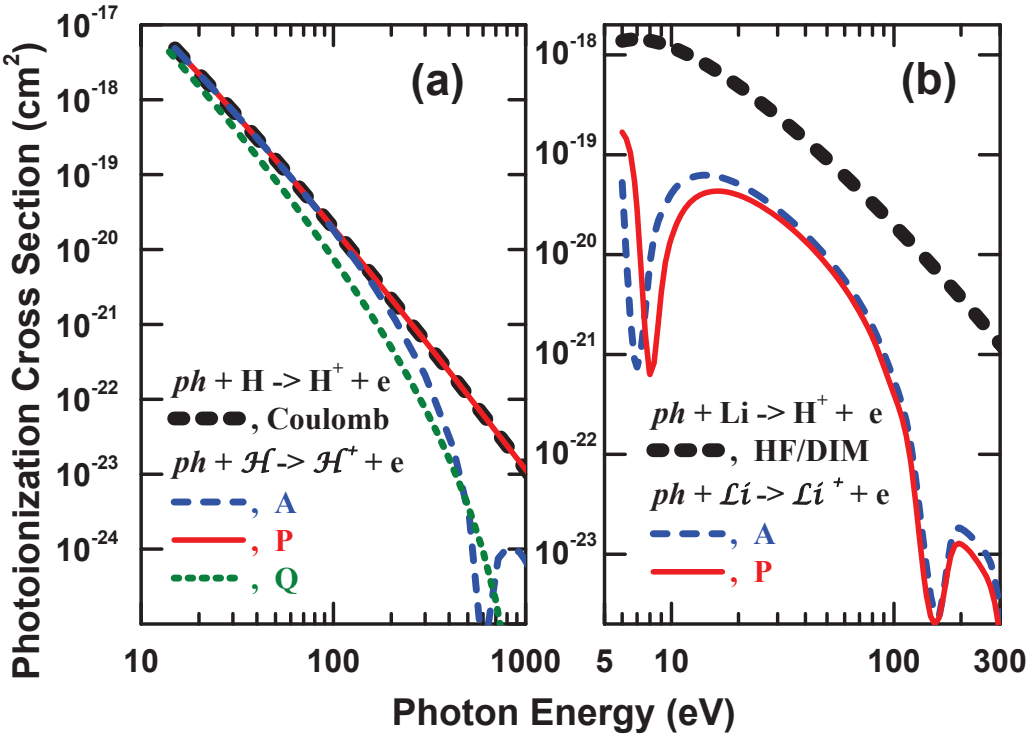

FIG. 4: (Color online) (a) Photoionization cross sections of hydrogen as a function of the photon energy in eV along with the ones obtained with PP. (b) similar to (a) for Lithium.

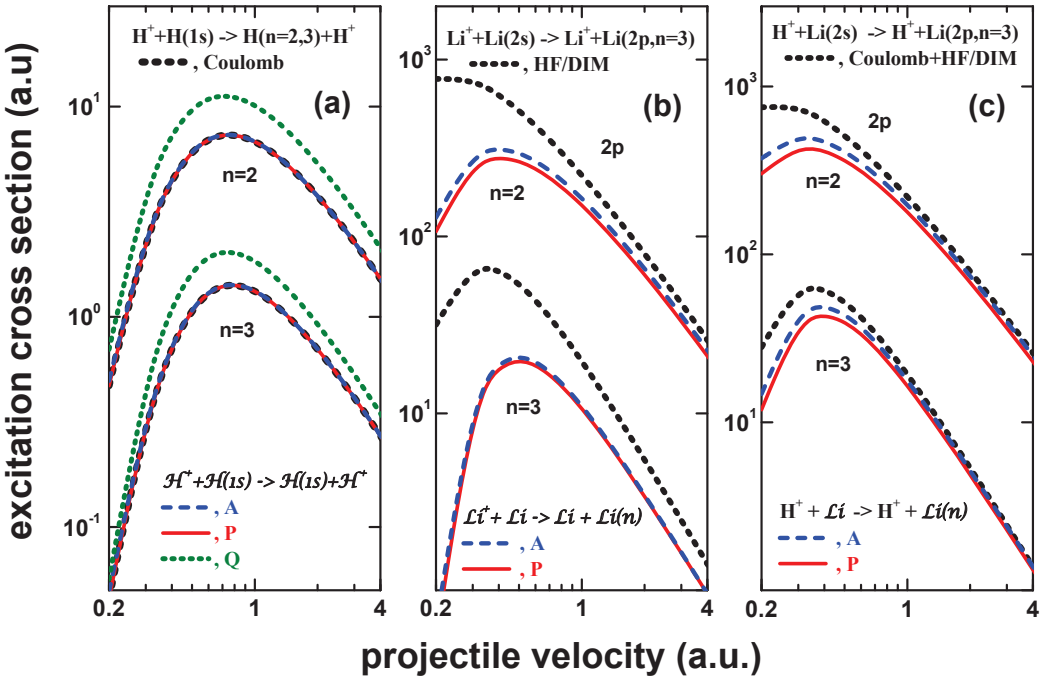

FIG. 5: (Color online) Excitation cross section as a function of the incident projectile velocity for hydrogen and pseudo hydrogen. (b) Similar to (a) for Lithium, as indicated. (c) Similar to (a) for impact of a bare hydrogen.

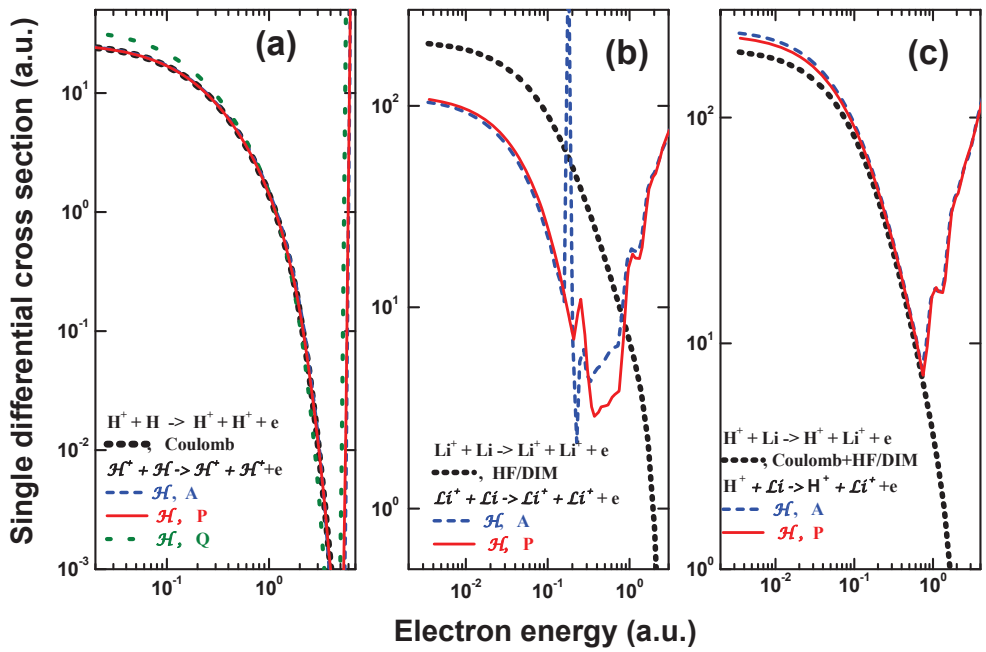

FIG. 6: (Color online) Ionization cross section as a function of the projectile velocity for hydrogen and pseudo hydrogen. (b) Similar to (a) for Lithium, as indicated. (c) Similar to (a) for impact of a bare hydrogen

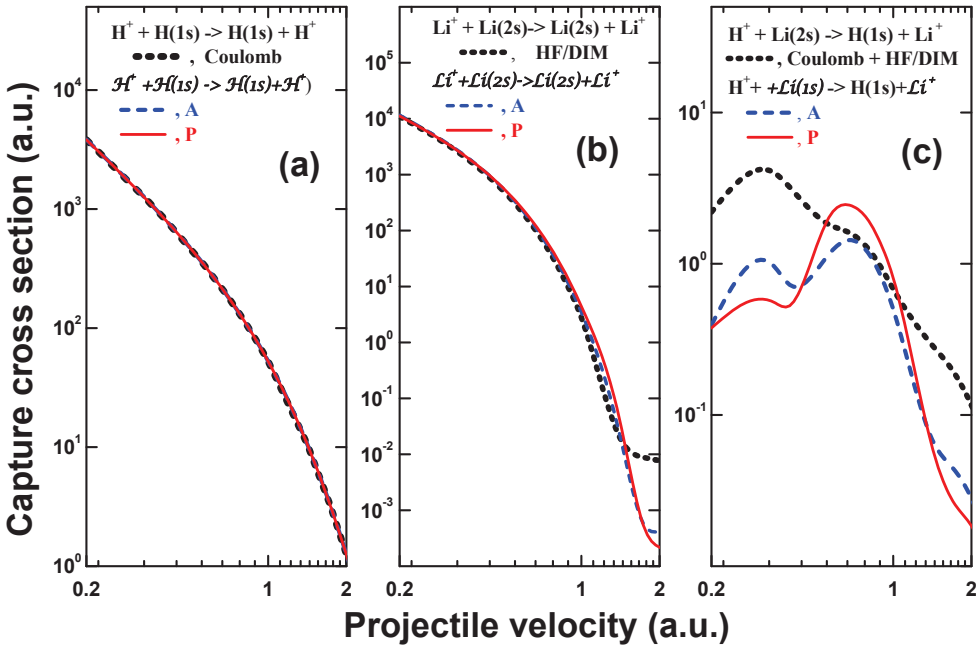

FIG. 7: (Color online) Electron capture cross section calculated in Brinkman Kramers approximations a function of the projectile velocity for hydrogen and pseudo hydrogen. (b) Similar to (a) for Lithium, as indicated. (c) Similar to (a) for impact of a bare hydrogen.